Mapping the paratope of anti-CD4 recombinant fab 13B8.2 by combining parallel peptide synthesis and site-directed mutagenesis

Cédric Bès, Laurence Briand-Longuet, Martine Cerutti, Frédéric Heitz, Samuel Troadec, Martine Pugnière, Françoise Roquet, Franck Molina, Florence Casset, Damien Bresson, et al.

THE JOURNAL OF BIOLOGICAL CHEMISTRY
Vol. 278, No. 16, Issue of April 18, pp. 14265–14273, 2003

Printed in U.S.A.

Mapping the Paratope of Anti-CD4 Recombinant Fab 13B8.2 by Combining Parallel Peptide Synthesis and Site-directed Mutagenesis*

Received for publication, October 18, 2002, and in revised form, January 27, 2003
Published, JBC Papers in Press, February 3, 2003, DOI 10.1074/jbc.M210694200

Cédric Bès‡§, Laurence Briant-Longuet¶, Martine Cerutti‖, Frédéric Heitz, Samuel Troadec‡, Martine Pugnière‡, Françoise Roquet‡, Franck Molina‡, Florence Casset‡‡, Damien Bresson‡, Sylvie Péraldi-Roux‡, Gérard Devauchelle‖, Christian Devaux¶, Claude Granier‡, and Thierry Chardès‖§§**

*From ‡CNRS UMR 5094, Institut de Biotechnologie et Pharmacologie, Faculté de Pharmacie, 15 Avenue Charles Flahault, 34093 Montpellier Cedex 5, France, ¶CNRS UMR 5121, Laboratoire Infections Rétrovirales et Signalisation Cellulaire, Institut de Biologie, 4 Boulevard Henri IV, 34060 Montpellier Cedex 2, France, ‖Institut National de la Recherche Agronomique-CNRS UMR 5087, Laboratoire de Pathologie Comparée, 30380 Saint-Christol-Lez-Alès, France, **CNRS UPR 1086, Centre de Recherche en Biochimie Macromoléculaire, 1919 Route de Mende, 34293 Montpellier Cedex 5, France, and ‡‡Synt:em, Parc Scientifique G. Besse, 30035 Nimes Cedex 1, France*

We analyzed antigen-binding residues from the variable domains of anti-CD4 antibody 13B8.2 using the Spot method of parallel peptide synthesis. Sixteen amino acids, defined as Spot critical residues (SCR), were identified on the basis of a 50% decrease in CD4 binding to alanine analogs of reactive peptides. Recombinant Fab 13B8.2 mutants were constructed with alanine residues in place of each of the 16 SCR, expressed in the baculovirus cell system, and purified. CD measurements indicated that the mutated proteins were conformationally intact, with a β-sheet secondary structure similar to that of wild-type Fab. Compared with the CD4-binding capacity of wild-type Fab 13B8.2, 11 light (Y32-L, W35-L, Y36-L, H91-L, and Y92-L) and heavy chain (H35-H, R38-H, W52-H, R53-H, F100K-H, and W103-H) Fab single mutants showed a decrease in CD4 recognition as demonstrated by enzyme-linked immunosorbent assay, BIAcore, and flow cytometry analyses. The five remaining Fab mutants showed antigen-binding properties similar to those of wild-type Fab. Recombinant Fab mutants that showed decreased CD4 binding also lost their capacity to inhibit human immunodeficiency virus promoter activation and the antigen-presenting ability that wild-type Fab displays. Molecular modeling of the 13B8.2 antibody paratope indicated that most of these critical residues are appropriately positioned inside the putative CD4-binding pocket, whereas the five SCR that were not confirmed by mutagenesis show an unfavorable positioning. Taken together, these results indicate that most of the residues defined by the Spot method as critical matched with important residues defined by mutagenesis in the whole protein context. The identification of critical residues for CD4 binding in the paratope of anti-CD4 recombinant Fab 13B8.2 provides the opportunity for the generation of improved anti-CD4 molecules with more efficient pharmacological properties.

The transmembrane glycoprotein CD4 is a major molecular partner in the immunological synapse that leads to optimal activation of T lymphocytes during immune responses (1). CD4 also serves as the primary receptor for the human immunodeficiency virus (HIV),[1] thereby allowing the virus to enter cells (2). At present, redesigned recombinant anti-CD4 antibodies (3–6) and a fully human anti-CD4 antibody from human immunoglobulin transgenic mice (7) are currently included in phase I–III trials for the treatment of autoimmune diseases, allograft rejection, and AIDS. We have expressed humanized anti-CD4 recombinant Fab 13B8.2 in the baculovirus/insect cell system, which is directed against the CDR3-like region of the D1 domain of CD4 (8). *In vitro*, this antibody prevents HIV transcription in $CD4^+$ cells at a post-gp120 binding step (8, 9) and also inhibits antigen presentation (8). Early phase I clinical trials (10–12) using the murine 13B8.2 antibody led to clinical benefits for some HIV-infected patients, *i.e.* disappearance of circulating p24 antigen (10, 12), no detectable reverse transcriptase activity (10), and generation of serum antibodies to gp120 and HIV-neutralizing antibodies (12).

The identification of critical residues from the antibody paratope involved in CD4 binding is a prerequisite for the improvement of such a recombinant antibody for future clinical trials. To this end, we previously characterized CD4-immunoreactive peptides in the 13B8.2 variable regions using the Spot method of parallel peptide synthesis (13). Whereas the Spot method has often been used to map interaction sites in epitopes (14), study of the antibody paratope (15) by probing overlapping peptides covering the variable regions of an antibody with labeled antigen was contrary to accepted dogma, probably due to the widely held view that the three-dimensional structure of the antibody is absolutely required for antigen binding. Initial experiments on defining residues critical for lysozyme binding in the HyHEL-5 antibody paratope (16) by the Spot method indirectly suggested that Spot critical residues (SCR) are involved in the "true" antibody paratope because ~65% of the identified SCR correlated with contributing residues previ-

* This work was supported in part by CNRS. The costs of publication of this article were defrayed in part by the payment of page charges. This article must therefore be hereby marked "*advertisement*" in accordance with 18 U.S.C. Section 1734 solely to indicate this fact.

§ Supported by fellowships from the Ministère de l'Education Nationale et de la Recherche and the Ensemble Contre le Sida.

§§ To whom correspondence should be addressed. Tel.: 33-467-548-604; Fax: 33-467-548-610; E-mail: thierry.chardes@ibph.pharma.univ-montp1.fr.

[1] The abbreviations used are: HIV, human immunodeficiency virus; CDR, complementarity-determining region; SCR, spot critical residue(s); mAb, monoclonal antibody; ELISA, enzyme-linked immunosorbent assay; PBS, phosphate-buffered saline; BSA, bovine serum albumin; IL-2, interleukin-2; L, variable region of the light chain; H, variable region of the heavy chain.

ously defined by x-ray crystallography of the lysozyme-HyHEL-5 complex (17, 18). Until now, no direct demonstration by simultaneous investigation using site-directed mutagenesis of the whole protein and Spot technology has shown that SCR from a given antibody actually belong to the paratope.

In this study on the mapping of key residues of Fab 13B8.2 involved in CD4 recognition, we first identified residues important for binding by the Spot approach; then, we used this information to design recombinant Fab 13B8.2 single mutants. These mutated recombinant molecules showed far-UV CD spectra similar to that obtained for wild-type Fab 13B8.2. Replacement of 11 of the 16 SCR with alanine resulted in impaired CD4 binding, thus confirming the results of the Spot antibody mapping. This impaired CD4 binding led to a loss of biological function of the recombinant Fab single mutants with respect to CD4-mediated immune responses. Based on a predicted three-dimensional model, all of these critical residues showed appropriate positioning inside the putative CD4-binding pocket. These results led to a view of the functional paratope of an anti-CD4 antibody and could further lead to a Spot-guided reshaping of anti-CD4 recombinant Fab 13B8.2.

EXPERIMENTAL PROCEDURES

Reagents, Cell Lines, and Vectors—CD4-inserted recombinant baculovirus was constructed and further used for the production of recombinant human soluble CD4 as described (8, 13). For Spot analysis, recombinant human CD4 (Repligen Inc., Needham, MA) was biotinylated using a commercial reagent (Amersham Biosciences) according to the manufacturer's instructions. The murine hybridoma cell line that produces mAb 13B8.2 (IgG1/κ) (10, 19) was kindly provided by Drs. D. Olive and C. Mawas (INSERM U119, Marseilles, France). The human lymphoblastoid B cell line EBV-Lu expressing HLA DR5/6, DRB52, DQ6/7, and A2 molecules and the murine T cell line pdb10F expressing human CD4 and pep24 (PAGFAILKCNNKTFNY)-specific chimeric T cell receptor (20) were a kind gift from Dr. P. De Berardinis (Consiglio Nazionale delle Ricerche, Napoli, Italy). The HeLa P4 HIV-1 long terminal repeat β-galactosidase indicator cell line (21) was provided by Dr. O. Schwartz (Institut Pasteur, Paris, France). The previously described (22) A2.01/CD4 T cell line expressing human wild-type CD4 was provided by Dr. D. Littman (New York University, New York).

Alanine Scanning of CD4-binding Peptides from the Variable Heavy and Light Chain Sequences of Fab 13B8.2—The general protocol for Spot peptide synthesis on cellulose membrane has been described (15). In 202 overlapping dodecapeptides frameshifted by one residue, corresponding to the deduced amino acid sequence of variable regions from the 13B8.2 antibody, anti-CD4 immunoreactivity was previously observed (13) for peptides including heavy chain sequences 31–41, 49–70, and 90–103 and light chain sequences 19–26, 32–40, and 85–96 (Kabat numbering). Seventeen hexapeptides covering those immunoreactive amino acid sequences and the six alanine analogs of each peptide were synthesized by the Spot method. Antigen reactivity of cellulose-bound peptides was assayed with biotinylated CD4 (1 μg/ml) under conditions that yielded a blue precipitate on reactive spots as described (13). The reactivity of the spots was evaluated by scanning the membrane and measuring the intensities of the spots with NIH Image Version 1.61 software. The SCR of the 13B8.2 paratope were identified on the basis of decreased antigen-binding capacity equal or superior to 50% of that of the unmodified peptide sequence.

Construction of Recombinant Baculoviruses Producing Anti-CD4 Wild-type or Alanine-mutated Fab 13B8.2—The general procedures concerning the cloning and sequencing of mAb 13B8.2 variable regions have been described (8, 13, 23). Site-directed mutagenesis of heavy or light chain genes from the 13B8.2 antibody was performed by overlapping PCR (24). The sixteen amino acids demonstrated to be SCR by alanine scanning analysis, two additional residues (Thr^{53} from the light chain and Val^{61} from the heavy chain) as controls, and Asn^{95} in the heavy chain were mutated to alanines. Each mutation was confirmed by automated DNA sequencing. For the preparation of heavy chain genes, the *Pst*I/*Sac*I-linearized variable heavy chain fragments were cloned into the plasmid cassette transfer vector pBHuFdγ_1, which contains the upstream pre-installed first domain of human Cγ_1 (Fdγ_1), allowing the insertion and expression of the 13B8.2 heavy chain under the control of the polyhedrin promoter (8, 25). For the preparation of light chain genes, the *Xho*I/*Kpn*I-linearized variable light chain fragments were cloned into the plasmid cassette transfer vector pBHuCκ, which contains the upstream pre-installed human Cκ gene (8, 25), allowing the insertion and expression of the 13B8.2 light chain under the control of the p10 promoter. A two-step recombination procedure (8, 25) was carried out to construct the recombinant baculoviruses, expressing both the heavy and light chains of wild-type or mutated Fab 13B8.2. Irrelevant anti-digoxin Fab 1C10 was expressed similarly in the baculovirus/insect cell system.

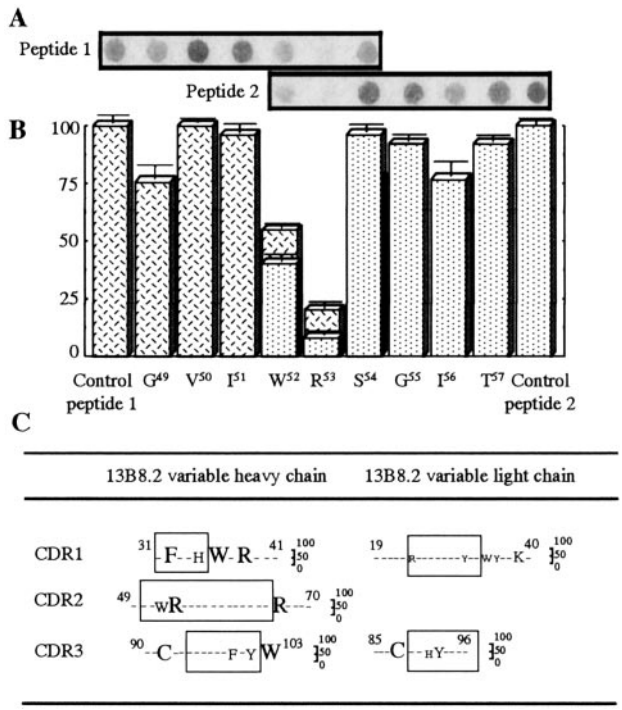

FIG. 1. **Determination by Spot alanine scanning of residues from the paratope of the 13B8.2 antibody contributing to CD4 binding.** *A*, scan of the CD4-probed membrane corresponding to control peptides 1 (^{49}GVIWRS^{54}) and 2 (^{52}WRSGIT^{57}) covering sequence 49–57 from the CDR-H2 region (Kabat numbering) and their respective sets of alanine hexapeptide analogs. *B*, quantitative analysis of the Spot reactivities of control peptides 1 (▨) and 2 (▩) covering sequence 49–57 from the CDR-H2 region. Each *bar* represents the reactivity of a hexapeptide whose sequence comprises Ala in place of the indicated amino acid. *C*, SPR from each CDR of the 13B8.2 variable heavy and light chains, measured by percent inhibition of CD4 binding (*vertical bars*). The percent inhibition is indicated by the size of the character. The CDR identification according to the Kabat nomenclature is *boxed*.

Recombinant Fab Production, Purification, and Characterization—Each recombinant Fab 13B8.2 mutant was protein G-immunopurified from a 400-ml supernatant of Sf9 cells (American Type Culture Collection CRL 1711) infected with recombinant baculovirus as previously described (8). Purified recombinant Fab was quantified by a sandwich ELISA using sheep anti-human Fdγ_1 antibody (The Binding Site, Birmingham, UK) as the capture reagent and peroxidase-conjugated anti-human κ light chain antibody (Sigma) as the detection reagent. Antibody samples were further checked for purity by electrophoresis and Western blot analysis.

Far-UV CD spectra were measured at 20 °C in 10 mM sodium phosphate buffer (pH 7.0) with a Jasco J-810 spectropolarimeter (Tokyo, Japan). The spectra represent an average of two scans recorded at a speed of 20 nm/min and a resolution of 0.1 nm. The antibody concentration was ~0.5 mg/ml. A cell with a 0.1-cm optical path length was used. Stability was characterized by further examination of the temperature dependence of the CD spectra in the range of 20–80 °C.

CD4 Binding Studies of Wild-type or Mutated Recombinant Fab 13B8.2—An ELISA method was performed to screen Fab 13B8.2 mutants for their ability to bind soluble CD4. A 1:500 dilution of the baculovirus-expressed CD4 fraction (8) in 0.1 M carbonate/bicarbonate buffer (pH 9.6) was coated overnight at 4 °C onto 96-well enzyme immunoassay plates (Nunc, Paisley, UK). Four washes with 160 mM PBS (pH 7.2) containing 0.1% Tween 20 (PBS/T) were performed before and after saturating plates in 1% nonfat powdered milk in PBS/T for 1 h at 37 °C. Thereafter, 100 μl of 2-fold serial dilutions of a 2.5 μg/ml

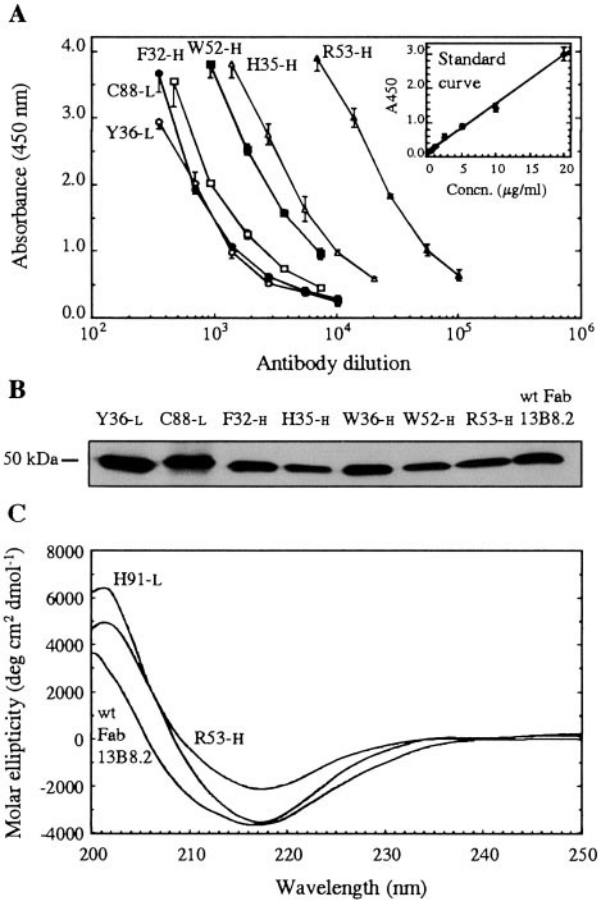

FIG. 2. **Characterization of alanine-mutated recombinant Fab 13B8.2 following protein G immunopurification from a baculovirus supernatant.** *A*, ELISA antibody titration curves for mutants Y36-L, C88-L, F32-H, H35-H, W52-H, and R53-H. *Inset*, the immunoglobulin standard curve. *B*, Western blot analysis of the 50-kDa Fab band revealed by peroxidase-conjugated anti-human κ light chain antibody. *C*, far-UV CD spectra of the H91-L and R53-H mutants *versus* wild-type (*wt*) Fab 13B8.2 in 10 mM phosphate buffer. *deg*, degrees.

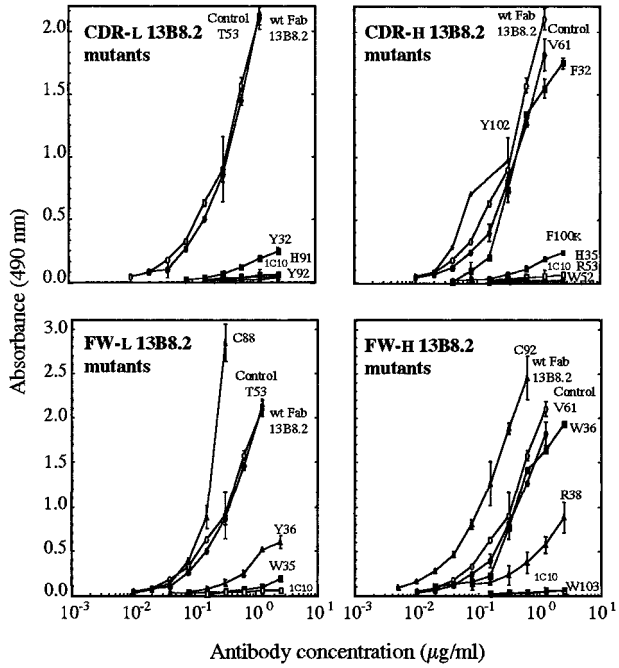

FIG. 3. **CD4 binding curves of various concentrations of alanine-mutated Fab 13B8.2 in comparison with wild-type Fab 13B8.2 and irrelevant Fab 1C10.** Each value represents the mean ± S.D. of triplicate determinations in an ELISA format. Results are representative of three independent experiments. *wt*, wild-type.

antibody solution was added to each well. Following incubation for 2 h and four washes with PBS/T, bound antibodies were detected by addition of 100 μl of a 1:1000 solution of peroxidase-conjugated anti-human κ light chain antibody, followed by subsequent addition of peroxidase substrate. Absorbance was measured at 490 nm. A similar ELISA experiment was performed to study the pH dependence of CD4 binding to wild-type Fab 13B8.2, except that the antibody was diluted in 0.2 M sodium phosphate buffer at various pH values, obtained by mixing different volumes of 0.2 M sodium dihydrogen phosphate and 0.2 M disodium hydrogen phosphate stock solutions.

The kinetic parameters of the binding of CD4 to Fab 13B8.2 were determined at 25 °C by surface plasmon resonance analysis using a BIAcore 2000 instrument (BIAcore AB, Uppsala, Sweden). Baculovirus-expressed CD4 was covalently immobilized on a CM5 sensor chip surface using the amine coupling method according to the manufacturer's instructions. A control reference surface was prepared using the same chemical treatment of the flow cell surface without injection of CD4. Recombinant Fab mutants in buffer containing 10 mM Hepes (pH 7.4), 3 mM EDTA, 150 mm NaCl, and 0.005% nonionic surfactant P20 (BIAcore AB) were then injected at concentrations between 5 and 20 μg/ml over the flow cell, and the dissociation phase was followed by a regeneration step with 5 mM HCl solution. The flow rate was 30 μl/min. All the sensorgrams were corrected by subtracting the low signal from the control reference surface. The data were globally fitted to a 1:1 Langmuir binding isotherm using BIAevaluation Version 3.2 software (26).

The binding of wild-type or mutated Fab to membrane CD4 was evaluated by flow cytometry. A2.01/CD4 T cells (1×10^6) were incubated with PBS containing 0.2% BSA (PBS/BSA) or with PBS/BSA supplemented with each recombinant Fab 13B8.2 mutant or irrelevant anti-digoxin Fab 1C10 expressed in the baculovirus/insect cell system. A similar experiment was performed with A2.01 T cells (a CD4-negative cell line). After three washes with PBS/BSA, bound antibodies were revealed by incubation of 50 μl of a 1:1000 dilution of fluorescein isothiocyanate-conjugated anti-human κ light chain antibody (Sigma) for 1 h at 4 °C. After three subsequent washes with PBS/BSA, the fluorescence intensity was measured on an EPICS cytofluorometer (Beckman-Coulter, Fullerton, CA).

IL-2 Secretion Assay following Antigen Presentation—Peptide-pulsed EBV-Lu antigen-presenting cells (10^5/well) were co-cultured with pdb10F responder T cells (2×10^4/well) as described (8, 13). Wild-type or mutated Fab 13B8.2 (20 μg/ml) was then added to the cells, which were subsequently cultured for 24 h at 37 °C. Thereafter, 100 μl of supernatant was harvested and tested for IL-2 secretion using a commercial ELISA kit (Pharmingen).

HIV-1 Promoter Activation Assay—HeLa P4 indicator cells (8×10^4/ml) were cultured in medium supplemented or not with infectious HIV-1_{Lai} in the presence or absence of Fab (20 μg/ml) for 3 days, harvested, and lysed. β-Galactosidase activity was then determined as previously described by measuring the absorbance at 410 nm (27).

Molecular Modeling of the Variable Regions of the 13B8.2 Antibody—A three-dimensional model of the variable heavy and light chains of the 13B8.2 antibody was obtained using the research version of the antibody modeling software A*b*M (Accelrys, Cambridge, UK) (28) running on an O2 R5000 Silicon Graphics work station. The CDR-L2, -L3, -H1, and -H2 loops were constructed using canonical class 1 frameworks and the CDR-L1 loop using a canonical class 2 framework, as defined by A*b*M. The CDR-H3 loop was built up using the combined data base/CONGEN search, a conformational generator program implemented in A*b*M, combined with a three-dimensional structural data base search. Hydrogens were added to the model using SYBYL software (Tripos Inc., St. Louis, MO), and the model was minimized during 100 iterations with the Tripos force field and the conjugate gradient method to eliminate all small steric conflicts. The solvent-accessible surface areas of 13B8.2 residues were calculated on the three-dimensional model by the SALVOL program (29) and implemented in SYBYL.

RESULTS

Identification by the Spot Method of Residues from the 13B8.2 Sequence Contributing to the Binding of CD4—Seventeen hexapeptides from previously identified antigen-binding sequences from the variable regions of the 13B8.2 antibody (13) and sets of alanine analogs were synthesized onto a cellulose membrane by the Spot method to identify antibody residues

TABLE I
BIAcore determination of the binding kinetics of the interaction between sensor chip-bound CD4 and 13B8.2 antibodies

Antibody	k_a	k_d	K_D
	$10^4\ M^{-1}\ s^{-1}$	$10^{-4}\ s^{-1}$	nM
Recombinant WT[a] Fab 13B8.2			
Exp. 1	0.3800 ± 0.080	1.08 ± 0.01	28.4 ± 0.70
Exp. 2	0.4800 ± 0.140	1.61 ± 0.02	33.5 ± 1.08
Exp. 3	0.2500 ± 0.007	0.64 ± 0.02	25.6 ± 1.30
Irrelevant Fab 1C10	NM	NM	NM
Fab 13B8.2 mutants			
Y32-L	0.0066 ± 0.001	5.85 ± 0.19	8863.6 ± 1650
W35-L			
Exp. 1	4.9400 ± 0.300	9.23 ± 0.09	18.7 ± 1.15
Exp. 2	6.6000 ± 0.200	8.41 ± 0.10	12.7 ± 0.43
Y36-L			
Exp. 1	2.5600 ± 0.003	6.51 ± 0.03	25.4 ± 1.38
Exp. 2	5.0000 ± 0.990	5.70 ± 0.12	11.4 ± 0.34
Control T53-L	2.2100 ± 0.080	3.65 ± 0.06	16.5 ± 0.65
C88-L	3.8000 ± 0.790	4.09 ± 0.09	10.8 ± 0.32
H91-L	0.0239 ± 0.002	40.40 ± 0.28	16,903.7 ± 1900
Y92-L			
Exp. 1	7.4700 ± 0.610	12.70 ± 0.03	17.0 ± 0.14
Exp. 2	7.0700 ± 0.030	8.89 ± 0.01	12.6 ± 0.06
F32-H			
Exp. 1	1.4400 ± 0.540	2.46 ± 0.07	17.1 ± 0.82
Exp. 2	1.4800 ± 0.310	2.50 ± 0.04	16.9 ± 0.44
H35-H	0.0301 ± 0.200	18.90 ± 0.85	6279.1 ± 4240
W36-H	1.7600 ± 0.470	2.71 ± 0.05	15.4 ± 0.52
R38-H	0.0163 ± 0.001	1.40 ± 0.03	858.9 ± 61.0
W52-H	0.0237 ± 0.008	8.59 ± 1.20	3624.5 ± 1420
R53-H	0.0359 ± 0.010	105.00 ± 1.45	29,247.9 ± 8400
Control V61-H			
Exp. 1	8.6800 ± 0.120	1.72 ± 0.03	2.0 ± 0.01
Exp. 2	11.2000 ± 0.800	3.24 ± 0.02	2.9 ± 0.02
C92-H	9.6100 ± 0.320	3.58 ± 0.02	3.7 ± 0.02
F100K-H	0.0562 ± 0.003	4.75 ± 0.05	845.1 ± 47.5
Y102-H	ND	ND	NC
W103-H	0.0278 ± 0.003	11.2 ± 0.27	4028.7 ± 567

[a] WT, wild-type; NM, not measurable; ND, not determined; NC, not calculated.

critically involved in CD4 binding. A detailed study of the reactivity of sequence 49–57 from the CDR-H2 region of the 13B8.2 antibody is shown as an example in Fig. 1 (*A* and *B*). Substituting Trp^{52} of peptide ^{49}GVIWRS^{54} (designated as control peptide 1) with alanine led to a 50% decrease in CD4-binding capacity, whereas changing Arg^{53} led to an almost complete loss of antigen reactivity. The four other alanine replacements in peptide ^{49}GVIWRS^{54} did not modify CD4-binding ability. The contribution of Trp^{52} and Arg^{53} to CD4 binding was confirmed by alanine scanning of peptide ^{52}WRSGIT^{57} (Fig. 1, *A* and *B*), designated as control peptide 2. Similar experiment using alanine analogs of hexapeptides ^{61}VPFMSR^{66} and ^{65}SRLSIT^{70} from the CDR-H2 region identified Arg^{66} as another CD4-binding residue (data not shown). Thus, the key residues from the H2 region were determined to be Trp^{52} and Arg^{53} (belonging to the CDR) and Arg^{66} (Fig. 1*C*).

In a similar manner, Phe^{32}, His^{35}, Trp^{36}, and Arg^{38} were determined by alanine scanning analysis of the three hexapeptides ^{31}TFGVHW^{36}, ^{34}VHWVRQ^{39}, and ^{36}WVRQSP^{41} from the H1 region of the 13B8.2 antibody, with two residues (Phe^{32} and His^{35}) being involved in the H1 region (Fig. 1*C*). The CD4-binding residues Cys^{92}, Phe^{100K}, Tyr^{102}, and Trp^{103} (Phe^{100K} and Tyr^{102} from CDR-H3 and the two other residues from frameworks) were determined from the three hexapeptides ^{90}YYCAKN^{95}, ^{92}CAKNDP^{97}, and ^{99}TGFAYW^{103} from the H3 region. Study of the four hexapeptides ^{19}VTFTCR^{24}, ^{21}FTCRAS^{26}, ^{32}YLAWYQ^{37}, and ^{35}WYQQKQ^{40} from the L1 region identified Arg^{24}, Tyr^{32}, Trp^{35}, Tyr^{36}, and Lys^{39} as contributing to CD4 binding. Because no reactivity was observed in the L2 region (13), no critical residue could be identified. The motif ^{88}C- -HY^{92} contributed to CD4 binding, as defined by Spot alanine scanning analysis of the three hexapeptides ^{85}TYYCQH^{90}, ^{88}CQHHYG^{93}, and ^{91}HYGNPP^{96} from the L3 region, with His^{91} and Tyr^{92} belonging to CDR-L3 (Fig. 1*C*). Taken together, 19 residues from the 13B8.2 variable heavy and light chain sequences were identified as contributing to CD4 binding by alanine scanning of previously identified CD4-binding peptides. These residues, defined on the basis of their importance in the Spot assay, were named SCR. However, among them, Arg^{66} from the heavy chain and Arg^{24} and Lys^{39} from the light chain were systematically found not to be accessible to the solvent in the three-dimensional structure of antibodies and have never been previously identified as critical residues for antigen binding (30, 31).[2,3] Therefore, only 16 SCR from the paratope of the 13B8.2 antibody were selected for further site-directed mutagenesis.

Characterization of Alanine-mutated Fab 13B8.2—The variable heavy and light chain genes from the 13B8.2 antibody were used as templates for overlapping PCR/site-directed mutagenesis to replace each identified SCR with an alanine residue in the Fab 13B8.2 context. Following cloning in the appropriate $pBHuFd_{\gamma 1}$ or pBHuCκ vector, expression in the baculovirus/insect cell system, and purification, each Fab alanine mutant (designated as F32-H, H35-H, W36-H, R38-H, W52-H, R53-H, C92-H, F100K-H, Y102-H, and W103-H for the heavy chain and Y32-L, W35-L, Y36-L, C88-L, H91-L, and Y92-L for the light chain) was further quantified by ELISA and characterized by Western blotting and far-UV CD. As exemplified for mutants Y36-L, C88-L, F32-H, H35-H, W52-H, and R53-H (Fig. 2*A*) using a sandwich ELISA format, Fab production could be demonstrated for each mutant. Coomassie Blue/

[2] Available at bioinf.org.uk/abs.
[3] Available at biochem.unizh.ch.

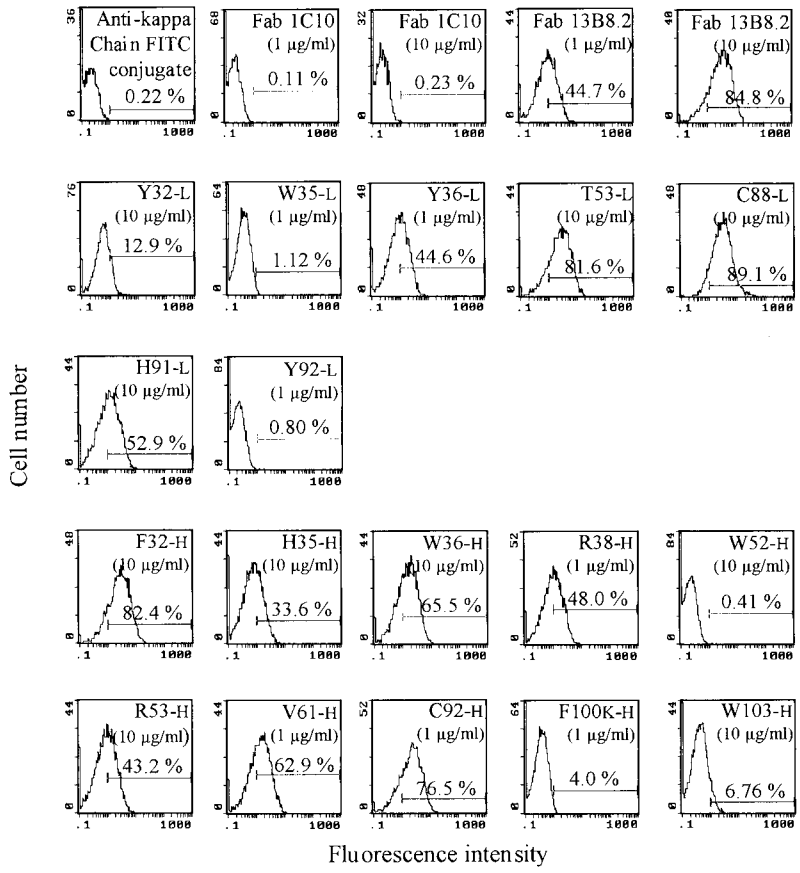

FIG. 4. **Flow cytometry analysis of the binding of each recombinant Fab 13B8.2 mutant *versus* wild-type Fab 13B8.2 and irrelevant Fab 1C10 to A2.01/CD4 T cells.** Results are representative of two different experiments. Antibody concentrations are indicated. *FITC*, fluorescein isothiocyanate.

SDS-PAGE of 1 μg of loaded protein for each recombinant revealed a single band at 50 kDa (data not shown), corresponding to the expected size of a correctly processed Fab fragment under nonreducing conditions. The identity of the 50-kDa band was confirmed by Western blotting using anti-human κ chain antibody (Fig. 2*B*). As exemplified for alanine-mutated Fab H91-L and R53-H, whose CD4-binding activities were the most drastically affected, a far-UV CD spectrum similar to that obtained for wild-type Fab was obtained for all mutants, with one negative peak at ~216 nm and one positive peak at ~200 nm (Fig. 2*C*). These results indicate that the mutated proteins we produced were conformationally intact, with a main β-sheet secondary structure similar to that of wild-type Fab 13B8.2. Furthermore, no modification of the spectra obtained with mutated proteins could be detected in the 20–80 °C temperature range (data not shown) in comparison with that obtained with wild-type Fab 13B8.2, suggesting that antibody stability was not affected by the mutations.

CD4-binding Ability of Alanine-mutated and Wild-type Fab 13B8.2—The ability of mutated *versus* wild-type Fab to bind soluble CD4 was first assessed by an ELISA method (Fig. 3) and then quantified by BIAcore analysis (Table I). In ELISA, the CD4-binding activity of wild-type Fab 13B8.2 was detectable in the 19.5–1250 ng/ml range (Fig. 3), whereas no binding was observed with irrelevant baculovirus-expressed anti-digoxin Fab 1C10. A CD4 dose-dependent reactivity similar to that found for wild-type Fab was demonstrated for control mutants T53-L and V61-H and also for alanine-mutated Fab C88-L, F32-H, W36-H, C92-H, and Y102-H. On the other hand, alanine mutation of Tyr^{32}, His^{91}, and Tyr^{92} from the CDR-L regions; His^{35}, Trp^{52}, Arg^{53}, and Phe^{100K} from the CDR-H regions; Trp^{35} and Tyr^{36} from the light chain frameworks; and Arg^{38} and Trp^{103} from their heavy chain counterparts affected CD4 binding in a dose-dependent manner (Fig. 3). These results were confirmed using BIAcore technology because most of the Fab mutants demonstrating a loss of CD4 binding by ELISA, *i.e.* Y32-L, H91-L, H35-H, R38-H, W52-H, R53-H, F100K-H and W103-H, showed a 100–1000-fold decrease in their K_D values, whereas those that maintained their CD4-binding ability by ELISA exhibited K_D values similar to that found for wild-type Fab 13B8.2 (Table I). Finally, mutants W35-L, Y36-L, and Y92-L, which showed a decrease in CD4 binding by ELISA, had K_D values resembling that of wild-type Fab 13B8.2, although with a higher dissociation rate.

To determine the binding of Fab 13B8.2 to membrane-bound CD4, antibody-labeled $CD4^+$ A2.01/CD4 T cells were analyzed by indirect immunofluorescence staining and flow cytometry (Fig. 4). Dose-dependent T cell staining was obtained with wild-type Fab 13B8.2, whereas control Fab 1C10 or fluorescein isothiocyanate-conjugated anti-human κ light chain antibody did not bind to the cells. Similar experiments conducted with CD4-negative A2.01 cells failed to show specific binding either with wild-type Fab 13B8.2 or its alanine mutants (data not shown). Alanine-mutated Fab Y36-L, C88-L, F32-H, W36-H, R38-H, and C92-H and control mutants T53-L and V61-H showed $CD4^+$ staining of A2.01/CD4 cells similar to that obtained with wild-type Fab. In contrast, a defect in CD4 binding was observed for mutants bearing alanine replacement of Tyr^{32}, Trp^{35}, His^{91}, and Tyr^{92} in the light chain and His^{35}, Trp^{52}, Arg^{53}, Phe^{100K}, and Trp^{103} in the heavy chain.

Biological Activities of Alanine-mutated Versus Wild-type Fab 13B8.2 on CD4-mediated Responses—pep24-pulsed EBV-Lu antigen-presenting cells co-cultured with pdb10F responder T cells led to IL-2 secretion following antigen presentation (20). As shown in Fig. 5, a dose-dependent inhibition of IL-2 secretion was demonstrated following incubation with anti-CD4 wild-type Fab 13B8.2 in this T cell activation model. At the same concentrations, control Fab 1C10 did not display any

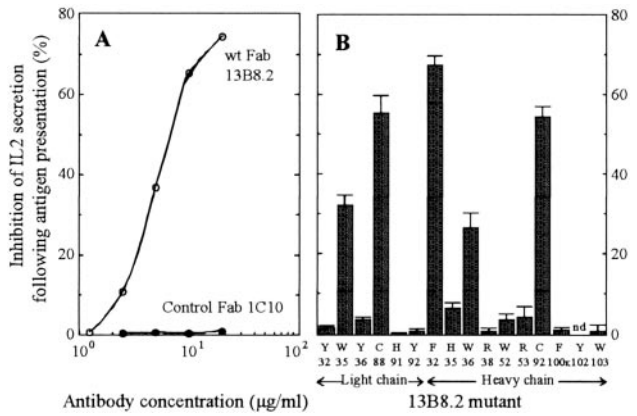

FIG. 5. **Inhibition of IL-2 secretion by pdb10f T cells sensitized with pep24-stimulated EBV-Lu antigen-presenting cells and co-cultured with recombinant Fab 13B8.2.** *A*, dose-response inhibition of IL-2 secretion by various concentrations of wild-type (*wt*) Fab 13B8.2 in comparison with irrelevant Fab 1C10. *B*, IL-2 secretion inhibition of each recombinant Fab 13B8.2 mutant. Mean absorbance at 450 nm varied from 0.015 for pdb10F cells co-cultured with unstimulated EBV-Lu antigen-presenting cells to 1.28 for pdb10F cells co-cultured with pep24-stimulated EBV-Lu antigen-presenting cells. A positive control for IL-2 secretion carried out by incubating murine anti-CD3 antibody (Pharmingen) with pdb10F T cells gave an absorbance of 2.30. *nd*, not determined.

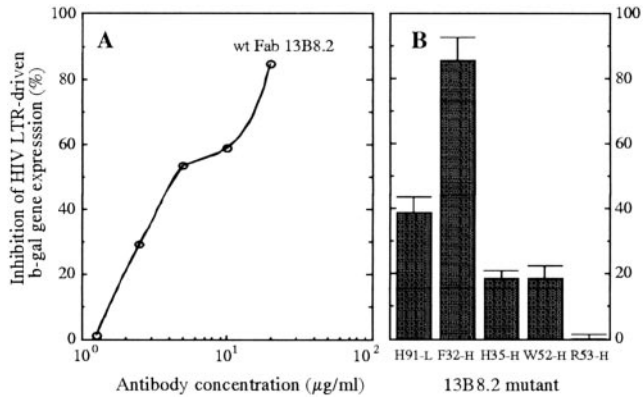

FIG. 6. **Inhibition of long terminal repeat-driven β-galactosidase gene expression induced by HIV-1_{Lai} following incubation with recombinant Fab 13B8.2.** *A*, dose-response inhibition of long terminal repeat (*LTR*)-driven β-galactosidase (*β-gal*) gene expression in HIV-1_{Lai}-infected HeLa P4 cells cultured in the presence of various concentrations of wild-type (*wt*) recombinant Fab 13B8.2. *B*, inhibition of β-galactosidase gene expression by recombinant Fab mutants H91-L, F32-H, H35-H, W52-H, and R53-H. Mean absorbance at 410 nm varied from 0.01 for uninfected indicator cells to 0.40 for HIV-1_{Lai}-infected indicator cells.

inhibitory activity. Mutants C88-L, F32-H, W36-H, and C92-H, which exhibited *in vitro* CD4-binding ability similar to that of wild-type Fab, also retained the wild-type inhibitory capacity in the antigen presentation test. In contrast, other mutations completely or partially abrogated the inhibition of the antigen-presenting function of the Fab (Fig. 5). This result correlated with those obtained in the study of the inhibitory property of Fab mutants H91-L, F32-H, H35-H, W52-H, and R53-H *versus* wild-type Fab on HIV-1 promoter activity (Fig. 6). In this case, Fab mutants showing impaired CD4-binding capacity (H91-L, H35-H, W53-H, and R53-H) were not able to block HIV-1 long terminal repeat-driven β-galactosidase reporter gene expression, whereas F32-H, with CD4-binding capacity similar to that of wild-type Fab 13B8.2, inhibited reporter gene expression. Taken together, mutations leading to impaired CD4 binding correlated with a defect in the biological activities of the Fab mutants.

Positioning Critical Residues on a Computer Model of the Variable Regions of the 13B8.2 Antibody—A three-dimensional model of the antibody paratope was obtained following the alignment of the amino acid sequence of mAb 13B8.2 with the A*b*M antibody sequence library (Fig. 7). The structure of 1fdl and 1nld antibodies provided the template for the 13B8.2 light and heavy chain frameworks, respectively. CDR conformations, except for CDR-H3, were predicted based on canonical classes. The most sequence-homologous known loops of the same canonical classes were used. CDR-L1, CDR-L2, and CDR-L3 were built using the three-dimensional 1fdl antibody structure, and CDR-H1 and CDR-H2 were built using the 1nld structure. The flexible CDR-H3 loop was not described as a canonical class and was built using a data base search combined with a conformational search (CONGEN). As expected, the structure presented two disulfide bridges, between Cys^{22} and Cys^{92} of the β-sheet of the heavy chain and between Cys^{23} and Cys^{88} of the β-sheet of the light chain.

When positioned on the 13B8.2 model, the SCR were found to fall into four groups depending on their location, solvent accessibility, and side chain orientation in the model, together with their true involvement as defined by site-directed mutagenesis (Fig. 7): group 1 (*red*) for well exposed SCR and group 2 (*pink*) for less accessible SCR, whose mutation affected CD4 reactivity; and group 3 (*blue*) for well exposed residues and group 4 (*turquoise*) for buried amino acids, whose mutant reactivity was not affected by site-directed mutagenesis.

Group 1 SCR (Tyr^{32}, His^{91}, and Tyr^{92} from the light chain and His^{35}, Trp^{52}, Arg^{53}, and Phe^{100K} from the heavy chain) are exclusively composed of basic and aromatic residues and are well located with great solvent accessibility and side chains oriented inside the CD4-binding pocket. Trp^{52} and Arg^{53} from the CDR-H2 loop and Tyr^{32} and Tyr^{92} from the CDR-L1 and CDR-L3 loops, respectively, are placed at the entrance of the antigen-binding site and are correctly positioned for CD4 binding. The bottom of the CD4-binding site is composed of a cluster of aromatic or positively charged residues: His^{35} and Phe^{100K} from the CDR-H1 and CDR-H3 loops, respectively, and His^{91} from the CDR-L3 region.

Group 2 SCR (Trp^{35} and Tyr^{36} from the light chain and Arg^{38} and Trp^{103} from the heavy chain) belong to the framework and are probably not directly involved in CD4 interaction (Fig. 7). These four additional residues, with less solvent accessibility, probably stabilize the backbone conformation of regions involved in the CD4-binding pocket or shape the variable heavy/light chain interface of the antibody. Although well located in the antibody paratope, one SCR (Phe^{32} from the heavy chain) belonging to group 3 points in a direction opposite to the main orientation of the CD4-binding pocket and was not confirmed by site-directed mutagenesis. Finally, group 4 SCR (Trp^{36} and Cys^{88} from the light chain and Cys^{92} and Tyr^{103} from the heavy chain) are clearly not involved in CD4 interaction because an alanine mutation in their Fab fragments did not affect CD4 binding, and they showed a side chain inaccessible to the solvent (Cys^{92}, Trp^{36}, and Cys^{88}) and/or were at a distance from the CD4-binding pocket, as for Tyr^{102} (Fig. 7). More specifically, the two cysteines are not accessible to the solvent and are involved in disulfide bridges, which might decrease their probability of interacting with CD4. Most of the amino acids mapped by the Spot approach and confirmed by site-directed mutagenesis are aromatic and/or charged residues. The presence of three critical positively charged residues lying at the entrance (Arg^{53} in CDR-H2) and the center (His^{35} in CDR-H1 and His^{91} in CDR-L3) of the CD4-binding site suggests that electrostatic interactions could be one major element of the binding between the 13B8.2 antibody and its epitope in the CDR3-like region of CD4. Indeed, CD4 binding to wild-type Fab 13B8.2 exhibited a pH depend-

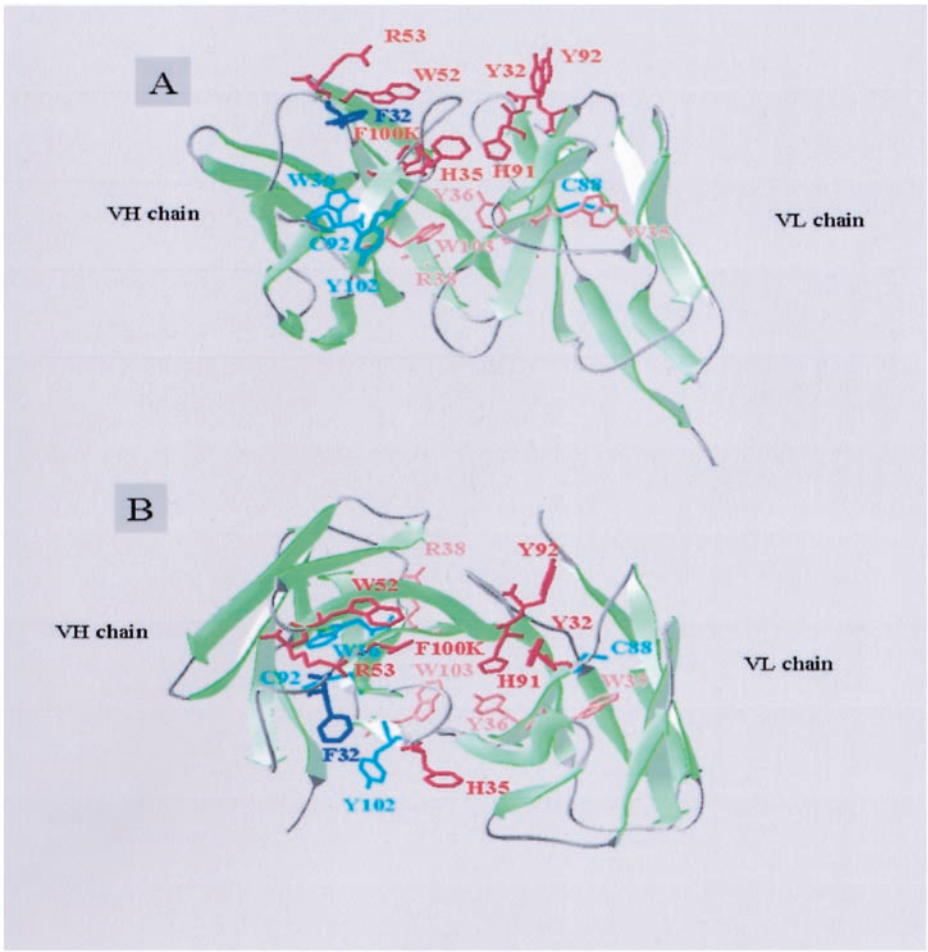

FIG. 7. **Three-dimensional model of the variable heavy and light chains of the 13B8.2 antibody generated using the A*b*M software, based on homology modeling (side (*A*) and top (*B*) views).** The model is shown with side chains for each selected SCR from the 13B8.2 paratope, using different colors relative to the SCR groups (*red* for group 1, *pink* for group 2, *blue* for group 3, and *turquoise* for group 4). SCR confirmed by site-directed mutagenesis experiments are in *red* and *pink*, whereas those not confirmed are in *blue* and *turquoise*. *VH*, variable heavy chain; *VL*, variable light chain.

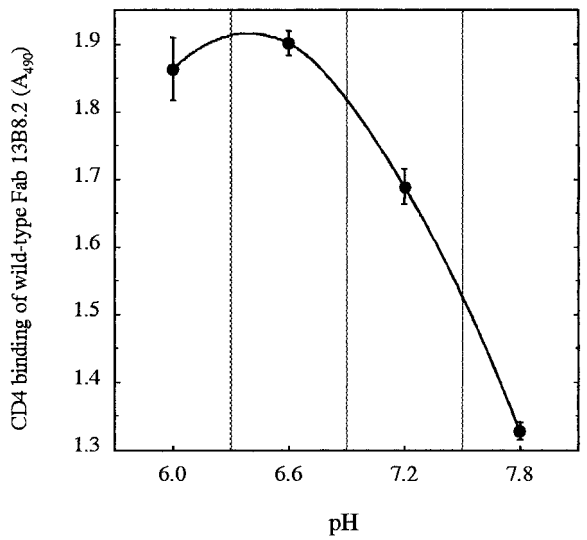

FIG. 8. **pH dependence of the binding of CD4 to Fab 13B8.2.** CD4 binding of a 10 μg/ml solution of wild-type Fab 13B8.2 (●) was analyzed by diluting the antibody fragment in 0.2 M sodium phosphate buffer at various pH values between 6.0 and 7.8. Each value represents the mean ± S.D. of triplicate determinations in an ELISA format.

ence (Fig. 8), arguing in favor of the role of positively charged residues in the 13B8.2 binding site. Finally, molecular modeling analysis of the CDR-L2 region showed that the L2 loop is relatively well exposed to the solvent, but structurally outside the antigen-combining site, thus explaining the reason why no CD4-binding activity was previously demonstrated by the Spot method (13).

DISCUSSION

The definition of critical residues involved in antigen binding from a given antibody paratope is a prerequisite for guiding the construction of a variant with improved activities. X-ray crystallography, sometimes combined with site-directed mutagenesis and/or molecular modeling, is the method of choice for delineating the antigen/antibody interface. Such analysis of the structural paratope is, however, limited to certain favorable cases, depending on the antibody and antigen availability, the level of antigen post-translational modifications, and the crystal quality of the complex, with these prerequisites being particularly critical for large proteins. Because of these difficulties, the atomic coordinates of antigen-antibody complexes from only ~20 different large proteins were available in December 2002 in the Protein Data Bank.

In this work, we used an approach based on the identification of residues critical for antigen binding by methods of parallel peptide synthesis combined with site-directed mutagenesis. Alanine scanning of previously defined CD4-binding peptides (13) from the 13B8.2 sequence mapped 16 amino acids whose mutation to alanine decreased peptide reactivity by >50%. Eleven CD4-binding residues as defined in the Spot format (SCR) were further confirmed to be directly or indirectly involved in the functional antibody paratope by site-directed mutagenesis experiments. Among them, 10 residues (Tyr^{32}, Trp^{35}, Tyr^{36}, His^{91}, and Tyr^{92} from the 13B8.2 light chain and His^{35}, Trp^{52}, Arg^{53}, Phe^{100K}, and Trp^{103} from the 13B8.2 heavy chain), which we defined as belonging to SCR groups 1 and 2, are in fact localized to positions of the antibody sequence corresponding to statistically frequent antigen contact residues (30, 31); four residues from SCR group 4, of the five excluded from the

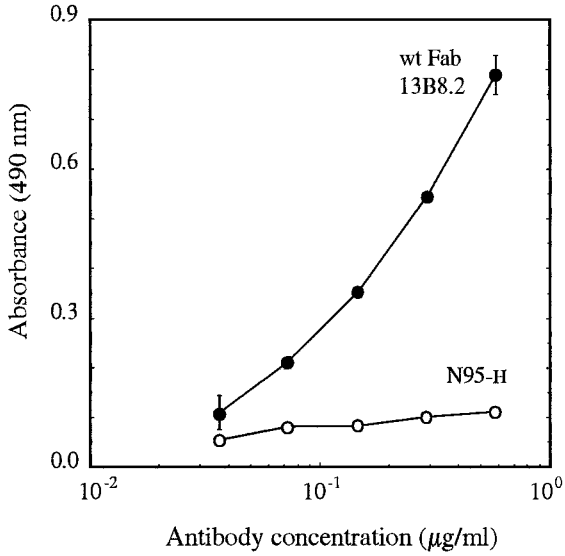

FIG. 9. **CD4 binding curves of various concentrations of alanine-mutated Fab N95-H on adsorbed CD4 in comparison with wild-type Fab 13B8.2.** Each value represents the mean ± S.D. of triplicate determinations in an ELISA format. Data are representative of three independent experiments. *wt*, wild-type.

CD4 paratope by the results of site-directed mutagenesis experiments, do not belong to this contact group. Interestingly, although located at a position belonging to the group of antigen contact residues (30, 31), Phe at position 32 of the heavy chain has never been retrieved as a critical amino acid (31). As we suggested in a previous study (15), the occurrence of false-positive SCR can be explained by the fact that the peptide format used to map the SCR allowed antibody residues normally buried in the folded paratope to be exposed. This is emphasized by the 13B8.2 modeling study, in which most of the SCR with no binding role were inappropriately oriented in the antigen-binding pocket, in accordance with the general view that the position and orientation of a residue relative to the center of the combining site are key points with respect to its propensity to bind antigen (30). Four critical residues from group 2 were found to be less accessible in the antigen-combining site model, but their mutations by site-directed mutagenesis affected CD4 binding, suggesting that they have an indirect influence on CD4 binding to the paratope. Among them, Trp^{35} and Tyr^{36} from the light chain and Trp^{103} from the heavy chain are located at positions belonging to the Vernier zone (32), which contains residues that adjust the CDR structure and fine-tune the fitting to antigen. Furthermore, amino acids at position 36 in the light chain and 103 in the heavy chain show a reduction of side chain-accessible surface upon formation of the dimer interface between the variable heavy and light chains (31), suggesting that they may be important for determining the shape of the antigen-binding pocket at the variable heavy/light chain interface.

One major question is how can interactions between an antigen and its combining site on the antibody be predicted from studies based on antigen interaction with cellulose-bound peptide fragments of the paratope? We can assume that probing such an overall interaction can be assimilated with the mapping of discontinuous epitopes by the Spot method (33, 34). In our case, the binding sites corresponding to the antigen-binding pocket were found to be distributed over most if not all of the CDR, located far apart in the primary structure, but brought together in the folded antibody to form the paratope. The complete paratope binds the antigen with high affinity, but individual binding sites from each CDR, corresponding to a peptide sequence, are probably characterized by a "degenerated" weak antigen interaction, which is much more difficult to identify. The Spot method can overcome such difficulty because high peptide density at each spot, in the range of 200–500 $nmol/cm^2$ (35), coupled with a very sensitive electrochemiluminescence detection system facilitates identification of weak binding peptides due to increased avidity for the probed antigen (36). In addition, several studies have demonstrated that some local flexibility contributes to antigen/antibody recognition, leading to conformational adaptation (37–40). C-terminally bound peptides on the cellulose membrane are unconstrained, as evidenced for peptides mimicking an interleukin-10 epitope (41), thus allowing high conformational flexibility, which could facilitate optimal positioning of key residues for binding. The binding conformation is thus "frozen" by the binding of the antigen. Finally, it has been reported (42) that the Spot method facilitates identification of binding site segments located in β-sheets inside the folded protein. Because the antibody structure is composed mainly of β-sheet elements, the Spot method is particularly appropriate for the identification of peptides and, in particular, their key residues involved in antigen binding.

Our observation that 13B8.2 mutants C88-L and C92-H expressed in the baculovirus/insect cell system still recognized CD4 and maintained biological properties deserves comments. Less than 1% of all variable region sequences have been described as lacking Cys at position 88 in the light chain or at position 92 in the heavy chain. Together with Cys^{23} from the light chain and Cys^{22} from the heavy chain, they form disulfide bonds between β-sheets to maintain thermodynamic stability and folding of the antibody. Whereas most of the cysteine-lacking recombinant antibodies expressed in bacteria demonstrated a defect in antigen-binding capacity, some active antibodies have been described, however, in eukaryotic systems (43). Our results might be explained by glutathione derivatization of the residual cysteine as described for yeast expression of the Cys-defective mutant lysozyme (44) or suggested for expression of Cys-defective whole antibodies (45).

We cannot exclude that other residues, mainly located in the CDR-H3 and CDR-L3 regions and not identified by the Spot method, contribute to CD4 binding. As suggested by computer-assisted 13B8.2 modeling analysis, Asn^{95} and Thr^{99} from the heavy chain and Asn^{94} from the light chain show a side chain orientation toward the center of the CD4-combining site (data not shown). In addition, they are located at positions defined as antigen contacts for the antibody (31). Preliminary ELISA experiments (Fig. 9) using alanine-mutated Fab N95-H argue in favor of such a contribution because no CD4 binding was observed for this mutant (<10% ELISA activity compared with wild-type Fab). Taken together, these observations outline the need to combine molecular modeling of the variable regions of a given antibody with 6-mer/12-mer Spot alanine scanning analysis of the paratope to accurately define critical residues for antigen binding.

Although no structure of any CD4-antibody complex has yet been described, molecular modeling of the OKT4A antibody, which recognizes an epitope in the CDR2-like loop of domain 1 of CD4, has permitted the study of its antibody combining site (4). Interestingly, some similarities between the binding pockets of the OKT4A and 13B8.2 antibodies can be noted. Two charged residues (Lys^{95} and Asp^{100A}) from the OKT4A heavy chain are centered in the binding site, which is also the case for the charged His^{35} and His^{91} residues from the heavy and light chains of mAb 13B8.2, respectively. The role of such positively charged residues from the 13B8.2 antibody must be underscored because (i) CD4 binding is increased by Fab 13B8.2

incubation at pH 6.0, at which 50% of the histidine residues are positively charged, but only 5% at pH 7.2; and (ii) the epitope of the 13B8.2 antibody mainly involves the negatively charged residues Glu^{87} and Asp^{88} on the CD4 molecule (46), suggesting that electrostatic interactions are of great importance in the 13B8.2 combining site. In a similar way, the two negatively charged critical residues from the OKT4A paratope (4) can interact with the positively charged Arg^{59} residue on the CD4 molecule, previously characterized as belonging to the epitope of the OKT4A antibody. Surrounding those residues, a cluster of aromatic side chain residues either from the 13B8.2 or OKT4A antibody essentially contribute to the binding. The bottom of the CD4-binding pocket involves more buried residues mainly belonging to the framework, such as Trp^{35}, Tyr^{36}, Arg^{38}, and Trp^{103} for the 13B8.2 antibody and Ala^{34}, Leu^{89}, Ser^{35}, and Ala^{50} for the OKT4A antibody, that may be critical for appropriately shaping the antigen-combining site (4). In addition, hydrogen bonding interactions between the main chain of His^{91} and the side chain of Tyr^{32} from the 13B8.2 light chain are suggested from our computational model to stabilize the CDR-L3 region, like those assessed by modeling analysis of the OKT4A antibody (between His^{49} from the light chain and Asp^{99} from the heavy chain) for stabilizing the CDR-H3 structure (4). On the basis of these arguments, we can speculate that similar interaction rules govern the binding of the 13B8.2 and OKT4A antibodies to their respective epitopes on the CD4 molecule, even if the induced biological responses are largely different.

The 13B8.2 antibody promotes post-entry inhibition of HIV transcription and T cell activation (2), such biological effects being abrogated using recombinant Fab harboring mutations impairing CD4 binding. In other words, these results indicate that at least His^{35}, Arg^{38}, Trp^{52}, Arg^{53}, Phe^{100K}, and Trp^{103} from the 13B8.2 heavy chain and Tyr^{32}, Trp^{35}, Tyr^{36}, His^{91}, and Tyr^{92} from the 13B8.2 light chain seem to be particularly critical in maintaining the desired biological effects of the 13B8.2 antibody. This set of data should be taken into consideration for the rational design of new anti-CD4 ligands of clinical value, derived either from recombinant Fab 13B8.2 (8) or from the CB1 paratope-derived peptide from the CDR-H1 region of the 13B8.2 antibody (13). A Spot-guided, site-directed mutagenesis of recombinant Fab 13B8.2 aimed at improving the activity of the 13B8.2 antibody can now be envisaged.

Acknowledgments—The skillful assistance of Verane Palumbo in the Spot synthesis of peptides is acknowledged. We thank Annick Ozil, Nicole Bres, Marylene Ozil, Sophie Boussinesq, Carine Charron, and Frederique Escuret for excellent technical assistance. We gratefully acknowledge Drs. D. Olive and C. Mawas for providing the mAb 13B8.2-producing cell line. We also thank Dr. Q. J. Sattentau for providing the CD4 cDNA-encoding plasmid, Dr. O. Schwartz for the HeLa P4 cell line, Dr. D. Littman for the A2.01/CD4 T cell line, and Dr. P. De Berardinis for the human lymphoblastoid B cell line EBV-Lu and the murine T cell line pdb10F. We are indebted to Dr. S. L. Salhi for editorial revision of the manuscript.

REFERENCES

1. Krummel, M. F., and Davis, M. M. (2002) *Curr. Opin. Immunol.* **14,** 66–74
2. Briant, L., and Devaux, C. (2000) *Adv. Pharmacol.* **48,** 373–407
3. Gorman, S. D., Clark, M. R., Routledge, E. G., Cobbold, S. P., and Waldmann, H. (1993) *Proc. Natl. Acad. Sci. U. S. A.* **88,** 4181–4185
4. Pulito, V. L., Roberts, V. A., Adair, J. R., Rothermel, A. L., Collins, A. M., Varga, S. S., Martocello, C., Bodmer, M., Jollife, L. K., and Zivin, R. A. (1996) *J. Immunol.* **156,** 2840–2850
5. Reimann, K. A., Lin, W., Bixler, S., Browning, B., Ehrenfels, B., Lucci, J., Miatkowski, K., Olson, D., Parish, T. H., Rosa, M. D., Oleson, F. B., Hsu, Y. M., Padlan, E. A., Letvin, N. L., and Burkly, L. C. (1997) *AIDS Res. Hum. Retroviruses* **13,** 933–943
6. Anderson, D., Chambers, K., Hanna, N., Leonard, J., Reff, M., Newman, R., Baldoni, J., Dunleavy, D., Reddy, M., Sweet, R., and Truneh, A. (1997) *Clin. Immunol. Immunopathol.* **84,** 73–84
7. Fishwild, D. M., O'Donnell, S. L., Bengoechea, T., Hudson, D. V., Harding, F., Bernhard, S. L., Jones, D., Kay, R. M., Higgins, K. M., Schramm, S. R., and Lonberg, N. (1996) *Nat. Biotechnol.* **14,** 845–851
8. Bès, C., Cerutti, M., Briant-Longuet, L., Bresson, D., Péraldi-Roux, S., Pugnière, M., Mani, J.-C., Pau, B., Devaux, C., Granier, C., Devauchelle, G., and Chardès, T. (2001) *Hum. Antib.* **10,** 67–76
9. Benkirane, M., Corbeau, P., Housset, V., and Devaux, C. (1993) *EMBO J.* **12,** 4909–4921
10. Dhiver, C., Olive, D., Rousseau, S., Tamalet, C., Lopez, M., Galindo, J. R., Mourens, M., Hirn, M., Gastaut, J. A., and Mawas, C. (1989) *AIDS* **3,** 835–842
11. Deckert, P. M., Ballmaier, M., Lang, S., Deicher, H., and Schedel, I. (1996) *J. Immunol.* **156,** 826–833
12. Schedel, I., Sutor, G. C., Hunsmann, G., and Jurkiewicz, E. (1999) *Vaccine* **17,** 1837–1845
13. Bès, C., Briant-Longuet, L., Cerutti, L., De Berardinis, P., Devauchelle, G., Devaux, C., Granier, C., and Chardès, T. (2001) *FEBS Lett.* **508,** 67–74
14. Frank, R. (1992) *Tetrahedron* **48,** 9217–9232
15. Laune, D., Molina, F., Ferrières, G., Villard, S., Bès, C., Rieunier, F., Chardès, T., and Granier, C. (2002) *J. Immunol. Methods* **267,** 53–70
16. Laune, D., Molina, F., Ferrières, G., Mani, J.-C., Cohen, P., Simon, D., Bernardi, T., Piechaczyk, M., Pau, B., and Granier, C. (1997) *J. Biol. Chem.* **272,** 30937–30944
17. Sheriff, S., Silverton, E., Padlan, E., Cohen, G. H., Smith-Gill, S., Finzel, B., and Davies, D. (1987) *Proc. Natl. Acad. Sci. U. S. A.* **84,** 8075–8079
18. Cohen, G. H., Sheriff, S., and Davies, D. R. (1996) *Acta Crystallogr. Sect. D Biol. Crystallogr.* **52,** 315–326
19. Corbeau, P., Benkirane, M., Weil, R., David, C., Emiliani, S., Olive, D., Mawas, C., Serres, A., and Devaux, C. (1993) *J. Immunol.* **150,** 290–301
20. Manca, F., De Berardinis, P., Fenoglio, D., Ombra, M. N., Li Pira, G., Saverino, D., Autiero, M., Lozzi, L., Bracci, L., and Guardiola, J. (1996) *Eur. J. Immunol.* **26,** 2461–2469
21. Briant, L., Robert-Hebmann, V., Acquaviva, C., Pelchen-Matthews, A., Marsh, M., and Devaux, C. (1998) *J. Virol.* **72,** 6207–6214
22. Poulin, L., Evans, L. A., Tang, S., Barboza, A., Legg, H., Littman, D. R., and Levy, J. A. (1991) *J. Virol.* **65,** 4893–4901
23. Chardès, T., Villard, S., Ferrieres, G., Piechaczyk, M., Cerutti, M., Devauchelle, G., and Pau, B. (1999) *FEBS Lett.* **452,** 386–394
24. Ho, S. N., Hunt, H. D., Horton, R., Pullen, J. K., and Pease, L. (1989) *Gene* (*Amst.*) **77,** 51–58
25. Poul, M.-A., Cerutti, M., Chaabihi, H., Devauchelle, G., Kaczorek, M., and Lefranc, M.-P. (1995) *Immunotechnology* (*Amst.*) **1,** 189–196
26. Karlsson, R., Roos, H., Fägerstam, L., and Persson, B. (1994) *Methods* (*Orlando*) **6,** 99–110
27. Monnet, C., Laune, D., Laroche-Traineau, J., Biard-Piechaczyk, M., Briant, L., Bès, C., Pugnière, M., Mani, J.-C., Pau, B., Cerutti, M., Devauchelle, G., Devaux, C., Granier, C., and Chardès, T. (1999) *J. Biol. Chem.* **274,** 3789–3796
28. Rees, A. R., Martin, A. C. R., Pedersen, J. T., and Searle, S. M. J. (1992) *AbM, a Computer Program for Modeling Variable Regions of Antibodies*, Oxford Molecular Ltd., Oxford, United Kingdom
29. Pearlman, R. S. (1991) *Natl. Inst. Drug Abuse Res. Monogr.* **112,** 62–77
30. MacCallum, R. M., Martin, A. C. R., and Thornton, J. M. (1996) *J. Mol. Biol.* **262,** 732–745
31. Honegger, A., and Plückthun, A. (2001) *J. Mol. Biol.* **309,** 657–670
32. Foote, J., and Winter, G. (1992) *J. Mol. Biol.* **224,** 487–499
33. Korth, C., Stierli, B., Streit, P., Moser, M., Schaller, O., Fisher, R., Schulz-Schaeffer, W., Kretzschmar, H., Raeber, A., Braun, U., Ehrensperger, F., Hornemann, S., Glockshuber, R., Riek, R., Billeter, M., Wüthrich, K., and Oesch, B. (1997) *Nature* **390,** 74–77
34. Reineke, U., Sabat, R., Misselwitz, R., Welfle, H., Volk, H.-D., and Schneider-Mergener, J. (1998) *Nat. Biotechnol.* **17,** 271–275
35. Kramer, A., Reineke, U., Dong, L., Hoffman, B., Hoffmüller, U., Winkler, D., Volkmer-Engert, R., and Schneider-Mergener, J. (1999) *J. Pept. Res.* **54,** 319–327
36. Reineke, U., Ivascu, C., Schlief, M., Landgraf, C., Gericke, S., Zahn, G., Herzel, H., Volmer-Engert, R., and Schneider-Mergener, J. (2002) *J. Immunol. Methods* **267,** 37–51
37. Foote, J., and Milstein, C. (1994) *Proc. Natl. Acad. Sci. U. S. A.* **91,** 10370–10374
38. Leder, L., Berger, C., Bornhauser, S., Wendt, H., Ackerman, F., Jelesarov, I., and Bosshard, H. R. (1995) *Biochemistry* **34,** 16509–16518
39. Davies, D. R., and Cohen, G. H. (1996) *Proc. Natl. Acad. Sci. U. S. A.* **93,** 7–12
40. Bosshard, H. R. (2001) *News Physiol. Sci.* **16,** 171–173
41. Welfle, K., Misselwitz, R., Sabat, R., Volk, H.-D., Schneider-Mergener, J., Reineke, U., and Welfle, H. (2001) *J. Mol. Recognit.* **14,** 89–98
42. Rüdiger, S., Germeroth, L., Schneider-Mergener, J., and Bukau, B. (1997) *EMBO J.* **16,** 1501–1507
43. Vrana, M., Tomasic, J., and Glaudemans, C. P. J. (1976) *J. Immunol.* **116,** 1662–1664
44. Taniyama, Y., Seko, C., and Kikuchi, M. (1990) *J. Biol. Chem.* **265,** 16767–16771
45. Proba, K., Honegger, A., and Plückthun, A. (1997) *J. Mol. Biol.* **265,** 161–172
46. Sattentau, Q. J., Arthos, J., Deen, K., Hanna, H., Healey, D., Beverley, P. C., Sweet, R., and Truneh, A. (1989) *J. Exp. Med.* **170,** 1319–1334